

# GaAs FET Ultrabroad-Band Amplifiers for Gbit/s Data Rate Systems

KAZUHIKO HONJO AND YOICHIRO TAKAYAMA

**Abstract**—A novel ultrabroad-band amplifier configuration suitable for GaAs FET's has been developed. The developed amplifier circuit operates as a capacitor-resistor ( $C$ - $R$ ) coupled amplifier circuit in the low-frequency range in which  $|S_{21}|$  for the GaAs FET's is constant. It also operates as a lossless impedance matching circuit in the microwave frequency range in which  $|S_{21}|$  for the GaAs FET has a slope of approximately  $-6$  dB/octave. Using this configuration technique, 800-kHz to 9.5-GHz band (13.5 octaves), 8.6-dB gain GaAs FET amplifier modules have been realized. The amplifier module has 40-ps step response rise time. It also has low input and output VSWR. By cascading two-amplifier modules, 19-dB gain over the 800-kHz to 8.5-GHz range and 50-ps step response rise time were obtained. NF is lower than 8 dB over the 50-MHz to 6-GHz range.

## I. INTRODUCTION

**S**IGNIFICANT advances in GaAs FET's have made it possible to realize gigabit systems. The gigabit-per-second data rate systems need amplifiers which exhibit flat gain of 20 dB or more over the frequency range from below several hundred kilohertz to above several gigahertz. In addition to these performances, low input and output voltage standing wave ratio (VSWR) is also required, especially for communication applications such as ultrahigh-speed pulse-code modulation (PCM) and optical communication systems.

A conventional approach to achieving these requirements is to use capacitor-resistor ( $C$ - $R$ ) coupled amplifier configuration, with feedback and/or peaking circuits, as the case may be.

Qualitative frequency-gain behaviors for the  $C$ - $R$  coupled amplifier, the  $C$ - $R$  coupled amplifier with the negative feedback circuit and the  $C$ - $R$  coupled amplifier with the peaking circuit are shown comparatively in Fig. 1.  $|S_{21}|$  of a conventional GaAs field-effect transistor (FET) having from 0.5- to 1.5- $\mu$ m gate length is constant below the frequency range from 0.5 to 2 GHz and exhibits a 6-dB/octave rolloff above that frequency range. Accordingly, the bandwidth of the simple  $C$ - $R$  coupled GaAs FET amplifiers, including direct coupled amplifiers, cannot be extended above about 2 GHz.

To achieve wider bandwidth, additional techniques, such as negative feedback and peaking techniques, have been used [1], [2]. However, there are two major disadvantages

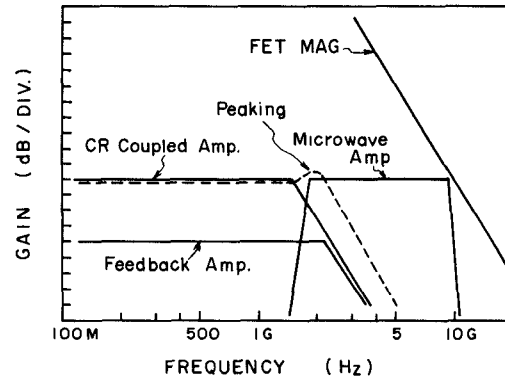


Fig. 1. Qualitative frequency-gain behaviors for a capacitor-resistor coupled amplifier, a peaking circuit, a negative feedback amplifier, and a microwave amplifier.

in negative feedback amplifiers. These are 1) degradation of amplifier gain, since the negative feedback amplifier has a constant value for gain-bandwidth product, and 2) added design difficulty in impedance matching. For the peaking technique, the bandwidth cannot be extended significantly since it is used in the  $C$ - $R$  coupled amplifier.

Meanwhile, as shown in Fig. 1, the gain of the  $C$ - $R$  coupled amplifier is low, compared with the maximum available gain (MAG) of the GaAs FET.

In conventional microwave amplifiers, lossless circuit elements such as lumped-element capacitors, inductors, and distributed transmission lines are usually used for impedances matching [3] or positive feedback [4] to achieve MAG at the upper band edge. However, not only do impedances for these lossless circuit elements depend upon frequencies, but also the number of sections of the matching network is limited from a practical point of view. Consequently, ultrabroad-band impedance matching using these lossless circuits is very difficult. Usually bandwidths for the broad-band multistage microwave amplifier are from 1 to 3 octaves. As a matter of fact, the bandwidths of these microwave amplifiers are too narrow to use for baseband pulse amplification in the gigabit data rate systems.

If the  $C$ - $R$  coupled amplifier low-frequency characteristics and the lossless matched microwave amplifier characteristics are combined, the GaAs FET high-frequency capability can be utilized to obtain a ultrabroad-band amplifier.

The purpose of this paper is to present a novel ultra-

Manuscript received November 4, 1980; revised January 26, 1981.

The authors are with the Basic Technology Research Laboratory, Nippon Electric Company, Ltd., 1-1, Miyasaki, Yonchome, Takatsu-ku, Kawasaki, Japan.

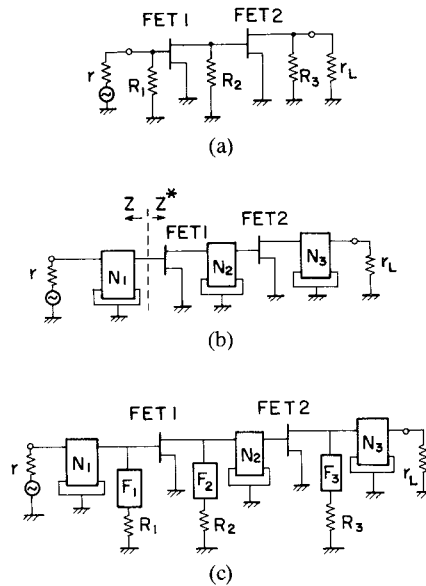


Fig. 2. Equivalent circuits for (a) conventional  $C$ - $R$  coupled amplifier; (b) conventional microwave amplifier; and (c) newly developed amplifier.

broad-band amplifier configuration suitable for GaAs FET's, and to demonstrate the performance of developed ultrabroad-band GaAs FET amplifiers. The novel amplifier circuit operates as the  $C$ - $R$  coupled amplifier circuit in the low-frequency range in which  $|S_{21}|$  for the GaAs FET's is constant. It also operates as the lossless impedance matching circuit in the microwave frequency range in which  $|S_{21}|$  for the GaAs FET's has a slope of approximately  $-6$  dB/octave. Using this circuit configuration, an 800-kHz to 9.5-GHz band, 8.6-dB gain amplifier module, in which 13.5-octave bandwidth has been achieved, has been developed. The amplifier module has 40-ps step response rise time. It also has low input and output VSWR. By cascading two amplifier modules, 19-dB gain over the 800-kHz to 8.5-GHz range and 50-ps step response rise time have been obtained. A 14-dB gain, 700-kHz to 6-GHz band amplifier module has also been developed. The noise characteristics are discussed.

## II. CIRCUIT DESIGN

### A. Configuration

An impedance matching technique for multistage amplifiers which have interstage matching networks is much more difficult than that for single-stage amplifiers. In order to obtain high gain, however, a multistage amplifier circuit configuration is necessary. Accordingly, design considerations have been made on two-stage amplifiers.

Schematic diagrams for a conventional  $C$ - $R$  coupled amplifier, a conventional microwave amplifier and a newly developed amplifier are shown in Fig. 2. In the figure, source grounded GaAs FET's are used. All coupling (dc blocking) capacitors and RF bypass capacitors are omitted for convenience, because these capacitors only affect a low-cutoff frequency. Fig. 2(a) shows the  $C$ - $R$  coupled amplifier which is generally used for baseband pulse

amplification. In the low-frequency range, the input impedances for source grounded GaAs FET's are very high, compared with the signal source impedance, which is usually  $50 \Omega$ . Accordingly, by selecting  $R_1$  to be  $r$ , low VSWR at the input port is achieved. Load resistance for the first stage FET (FET 1) is decided mainly by  $R_2$ . Considering the output impedance for the second-stage FET (FET 2),  $R_3$  is chosen to achieve low VSWR at the output port. Load resistance for the amplifier  $r_L$  is usually  $50 \Omega$ .

Fig. 2(b) shows a typical two-stage microwave amplifier using lossless low-pass impedance matching networks  $N_1$ ,  $N_2$ , and  $N_3$ . The impedance is matched to obtain MAG at the upper band edge.

Fig. 2(c) shows a newly developed amplifier schematic diagram. In the figure,  $N_1$ ,  $N_2$ , and  $N_3$  are low-pass lossless impedance matching networks, and  $F_1$ ,  $F_2$ , and  $F_3$  are low-pass lossless impedance transformers. Resistors  $R_1$ ,  $R_2$ , and  $R_3$  have the same values, respectively, as in Fig. 2(a) and  $N_1$ ,  $N_2$ , and  $N_3$  have the same values, respectively, as in Fig. 2(b). By means of transformers  $F_1$ ,  $F_2$ , and  $F_3$ , resistors  $R_1$ ,  $R_2$ , and  $R_3$  are transformed into high impedances in the microwave frequency range so that these resistors do not affect microwave impedance matching. The microwave impedance matching is achieved by  $N_1$ ,  $N_2$ , and  $N_3$ , just like the circuit in Fig. 2(b). Meanwhile,  $N_1$ ,  $N_2$ ,  $N_3$ ,  $F_1$ ,  $F_2$ , and  $F_3$  in Fig. 2(c), which are all low-pass form elements, operate as circuits having short electrical length in the low-frequency range. The low-frequency range gain is determined by  $R_1$ ,  $R_2$ , and  $R_3$ .

Amplifier gains both in the low-frequency range and in the microwave frequency range can be established individually. To apply the circuit to flat-gain ultrabroad-band amplifiers, the gains in both frequency ranges are designed to be the same. A gain ripple which may occur in a crossover frequency range between the low and the microwave frequency ranges can be flattened by proper design

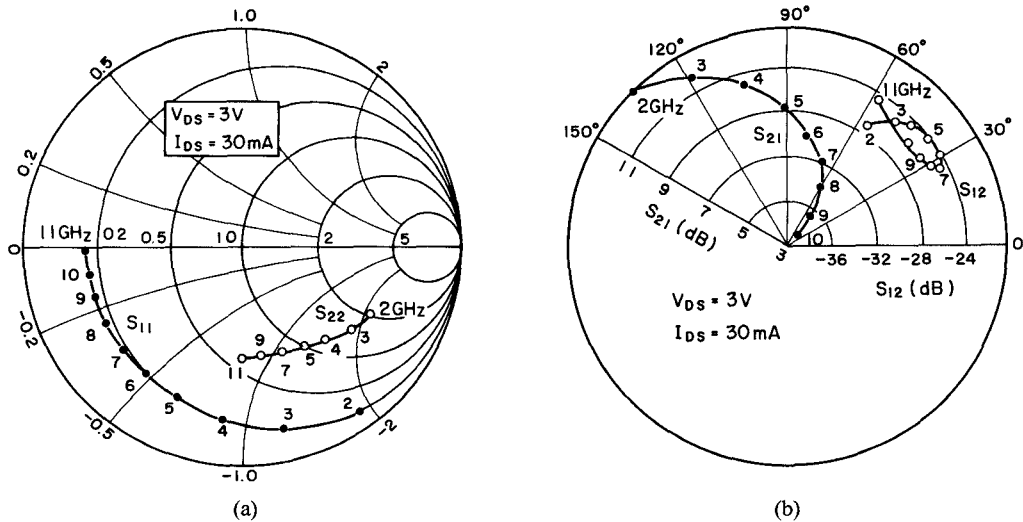


Fig. 3. S parameters for V-218 FET. (a)  $S_{11}$  and  $S_{22}$ . (b)  $S_{12}$  and  $S_{21}$ .

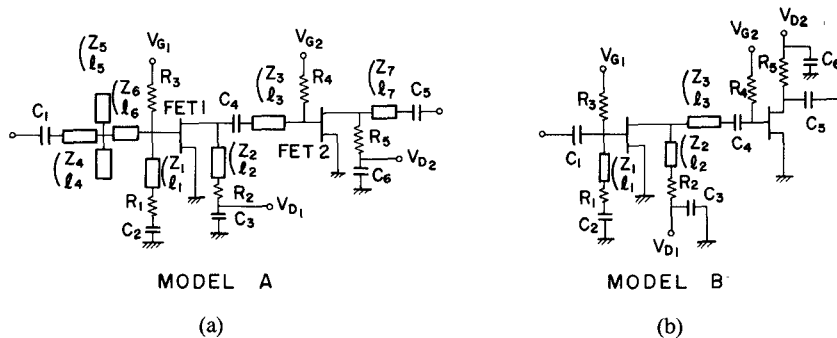


Fig. 4. Equivalent circuits for amplifier modules. (a) Model A. (b) Model B.

TABLE I  
DESIGNED CIRCUIT PARAMETERS FOR MODEL A AND MODEL B

	$(\Omega)$				$(\Omega)(\text{mm})$							$(\text{pF})$	
	$R_1$	$R_2$	$R_3, R_4$	$R_5$	$Z_1/l_1$	$Z_2/l_2$	$Z_3/l_3$	$Z_4/l_4$	$Z_5/l_5$	$Z_6/l_6$	$Z_7/l_7$	$C_1, C_4, C_5$	$C_2, C_3, C_6$
Model A	50	37	3000	75	100/1.7	100/1.7	48/1.6	26/5.2	40/1.4	100/1.7	100/0.5	3300	21300
Model B	50	50	3000	300	100/5	100/4	33/5.6	—	—	—	—	3300	21300

using a computer simulation. The simulation results are demonstrated in the next section.

**B. Ultrabroad-Band Amplifier Module Design**

The GaAs FET's used in the amplifier modules are V-218 FET's (NEC). The FET gate length and total gate width are 1.0 and 400  $\mu\text{m}$ , respectively. The FET has two-cell and recessed gate structure. Saturated drain current  $I_{DSS}$  is 120-mA and pinchoff voltage  $V_p$  is  $-2.2$  V.

S parameters for a V-218 FET are shown in Fig. 3. The S parameters in the figure are extracted using the FET equivalent circuit element values which are determined by computer data fitting techniques for the measured S parameters.

Two categories (Model A and Model B) of amplifier modules were designed. Equivalent circuits for the Model

A and the Model B are shown in Figs. 4(a) and (b), respectively.

Model A was designed to have a wider bandwidth but a lower gain compared to Model B. Using microstrip line type single section impedance transformers, the low-pass transformers ( $F_1$ ,  $F_2$ , and  $F_3$ ) in Fig. 2(c) are realized. Microstrip lines and stubs are also adopted for input, interstage and output low-pass matching networks ( $N_1$ ,  $N_2$ , and  $N_3$ ).

$F_3$  in Fig. 2(c) is omitted in Model A and  $N_1$ ,  $N_3$ , and  $F_3$  in Fig. 2(c) are omitted in Model B. Resistances  $R_3$  and  $R_4$  in gate bias voltage supply circuits are high enough not to affect the low frequency and the microwave circuits.  $C_1$ ,  $C_4$ , and  $C_5$  are coupling (dc blocking) capacitors.  $C_2$ ,  $C_3$ , and  $C_6$  are RF bypass capacitors. Designed circuit parameters are shown in Table I.

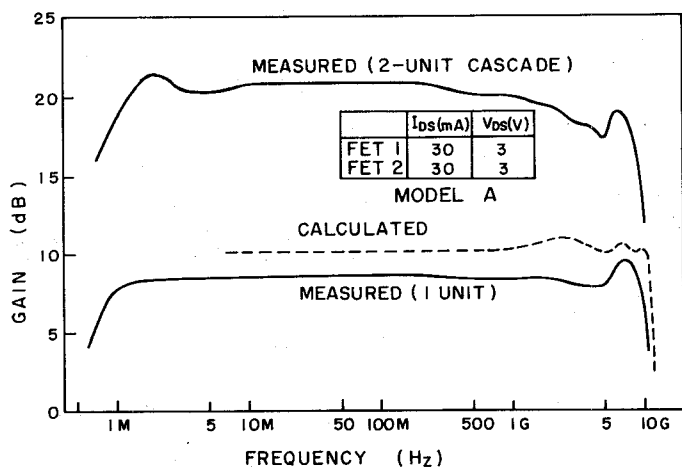


Fig. 5. Gain-frequency characteristics for the Model A amplifier module and the cascade amplifier.

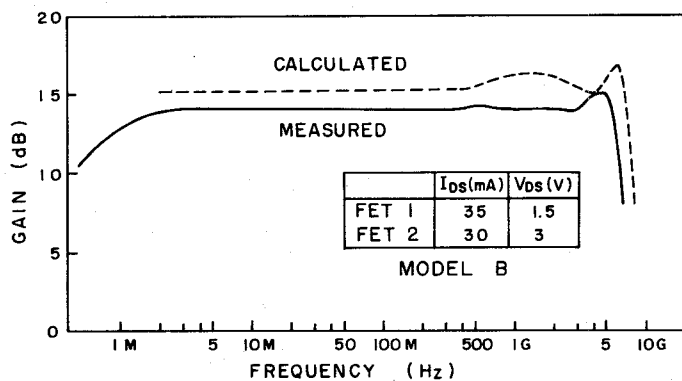


Fig. 6. Gain-frequency characteristics for the Model B amplifier module.

A simulated frequency-gain characteristic for the Model A amplifier module is shown in Fig. 5. That for the Model B amplifier module is shown in Fig. 6. As shown in the figures, the Model A amplifier module band reaches 10.5 GHz with 10-dB gain and the Model B amplifier module band reaches 7 GHz with 15-dB gain. Low-cutoff frequencies of the amplifier modules are due to the coupling capacitors. For the matching network design in the microwave frequency range, computer-aided design optimization was used.

C. Circuit Description

Photographs of Model A and Model B amplifier modules are shown in Fig. 7. Coupling and RF bypass capacitors are multilayer high dielectric constant ceramic capacitors. These capacitors were tested in a 50-Ω system, in advance, over the 2-GHz to 8-GHz range. The VSWR for these capacitors is less than 1.5 over the frequency range. Resistors and microstrip lines are fabricated on 0.635-mm thick alumina ceramic plates having a Au-Cr-Ta<sub>2</sub>N metal system. The rated sheet resistance for the Ta<sub>2</sub>N film is 50 Ω.

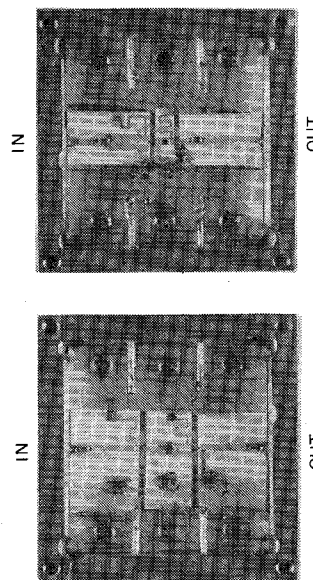


Fig. 7. Amplifier module photographs. (a) Model A. (b) Model B.

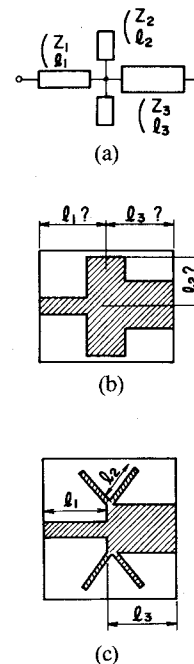


Fig. 8. Equivalent circuit and configurations for an input microwave matching network. (a) Equivalent circuit. (b) Conventional configuration. (c) Configuration used in this paper.

Fig. 8 shows an equivalent circuit for an input microwave matching circuit in Model A, and two microstrip configurations for the equivalent circuit. In the circuit configuration in Fig. 8(b), when microstrip-conductor widths of the stubs are not negligibly narrow compared with the microstrip line lengths (characteristic impedances for the stubs are low), it is difficult to realize equivalent electrical angles  $\gamma l_1$ ,  $\gamma l_2$ , and  $\gamma l_3$  (where  $\gamma$  is propagation constant) which are shown in Fig. 8(a).

Y parameters for a transmission line having characteris-

tic impedance  $Z_0$ , propagation constant  $\gamma$ , and length  $l$  are given by

$$(Y) = \begin{pmatrix} \frac{\cosh \gamma l}{Z_0 \sinh \gamma l} & -1 \\ -1 & \frac{\cosh \gamma l}{Z_0 \sinh \gamma l} \end{pmatrix}. \quad (1)$$

Accordingly,  $Y$  parameters ( $Y_n$ ) for  $n$  parallel transmission lines are calculated as

$$(Y_n) = \begin{pmatrix} \frac{\cosh \gamma l}{(Z_0/n) \sinh \gamma l} & -1 \\ -1 & \frac{\cosh \gamma l}{(Z_0/n) \sinh \gamma l} \end{pmatrix} \quad (2)$$

where  $n$  is a positive integer.

As shown in (2), the  $n$  parallel transmission lines for characteristic impedance  $Z_0$  are equivalent to a transmission line with characteristic impedance  $Z_0/n$ , having the same line length. The relation between microstrip-conductor width  $W$  for characteristic impedance  $Z_0$  and strip conductor width  $W_n$  for characteristic impedance  $Z_0/n$  is as shown in the following:

$$\frac{W}{W_n} \ll \frac{1}{n}.$$

By substituting a stub with characteristic impedance  $Z_2$  and length  $l_2$  by two parallel stubs with characteristic impedance  $Z_2/2$  and length  $l_2$ , the sum of microstrip-conductor widths for the stubs can be reduced. Therefore, the circuit configuration in Fig. 8(c) is more suitable than that in Fig. 8(b), for the stubs having low characteristic impedances. All circuit components were mounted on a metal carrier measuring 3 cm  $\times$  3 cm.

#### IV. PERFORMANCE

##### A. Frequency-Domain Characteristics

The gain-frequency characteristic measured in a 50- $\Omega$  system for the Model A amplifier module is shown in Fig. 5. An 8.6-dB gain is obtained over the 3-dB bandwidth from 800 kHz to 9.5 GHz. A 13.5-octave bandwidth is achieved. Fig. 9 shows input and output VSWR for the 800-kHz to 9.5-GHz amplifier module. The input VSWR is lower than 2 over the 2-MHz to 1-GHz range and is lower than 4 over the 1-MHz to 10-GHz range. For the output VSWR, less than 2 can be obtained over the 2-MHz to 9-GHz range. Input-output power responses for the amplifier module, measured at 0.5 GHz, 1 GHz, 4 GHz, and 8 GHz, are shown in Fig. 10. The amplifier module has a 12-dBm power output at 1-dB gain compression over the frequency range, from 0.5 GHz to 8 GHz.

Gain-frequency characteristic for the Model B amplifier module is also shown in Fig. 6. A 14-dB gain is obtained over the 3-dB bandwidth from 700 kHz to 6 GHz. For pulse amplifications, a linear phase (nondispersive) char-

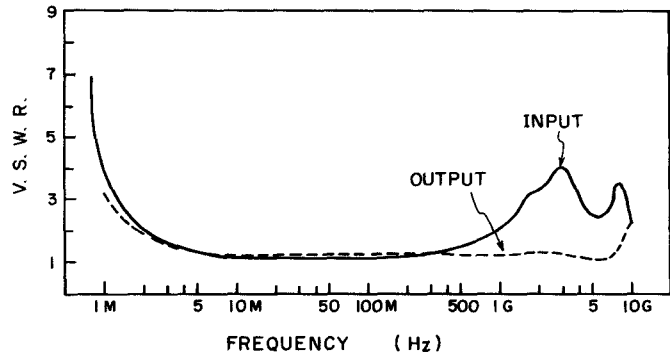


Fig. 9. Input and output VSWR for the 800-kHz to 9.5-GHz amplifier module.

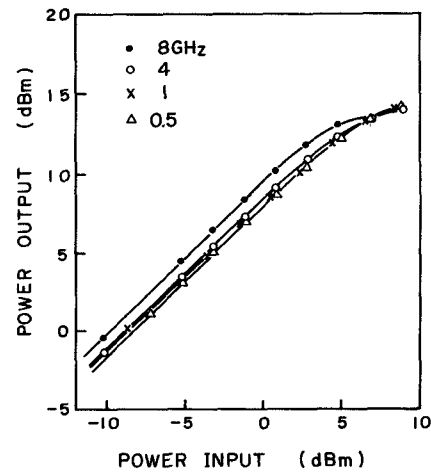


Fig. 10. Input-output power response for 800-kHz to 9.5-GHz amplifier module.

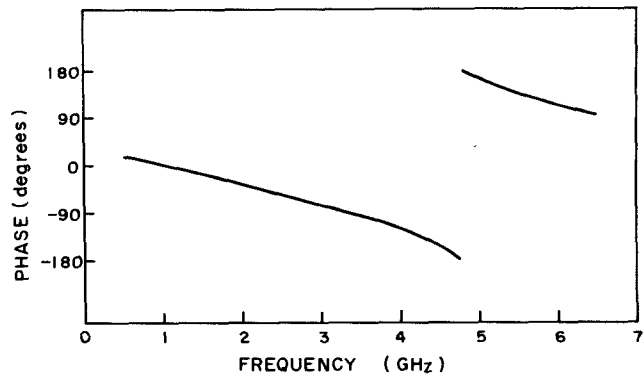


Fig. 11. Phase-frequency characteristic for Model B amplifier module.

acteristic as well as a flat-gain characteristic are required. Fig. 11 shows a measured phase-frequency characteristic for the Model B amplifier module. As seen in the figure, the amplifier modules has approximately linear phase across the frequency band.

By cascading two 800-kHz to 9.5-GHz amplifier modules without any external matching, 19-dB gain is obtained over the 800-kHz to 8.5-GHz band. The result is also

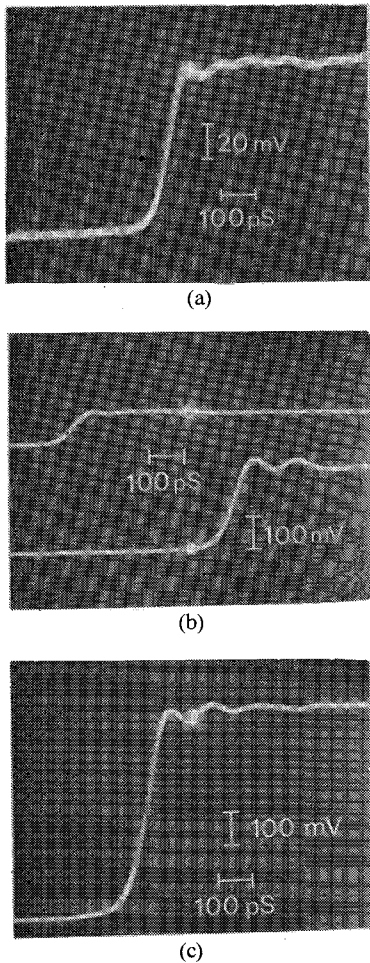


Fig. 12. Step responses for the 800-kHz to 9.5-GHz amplifier module and the cascade amplifier. (a) Input waveform. (b) Input and output waveforms for the module. (c) Output waveform for the cascade amplifier.

shown in Fig. 5. The gain-frequency characteristic has a slight gain slope caused by  $R_2$  of the second amplifier module. The  $R_2$  value measured for the fabricated second amplifier module was higher than the designed value. Adjusting the  $R_2$  value lower, so that the gain of the low-frequency range is reduced a flat gain will be achieved. The experimental result for the cascade amplifier demonstrates that, by cascading the amplifier modules, higher gain can be obtained without serious bandwidth degradation.

### B. Time-Domain Characteristics

Step responses for the 800-kHz to 9.5-GHz amplifier module and the cascade amplifier are shown in Fig. 12. Fig. 12(a) shows the input waveform having a 10-percent to 90-percent rise time of 75 ps. Both input and output waveforms for the 800-kHz to 9.5-GHz amplifier module are shown in Fig. 12(b). The input waveform is the same as in Fig. 12(a). Rise time for the output waveform is 85 ps. A well-known approximate relation involving real step response rise time for the amplifier output  $t_a$  measured rise time for the input waveform  $t_i$  and measured rise time for

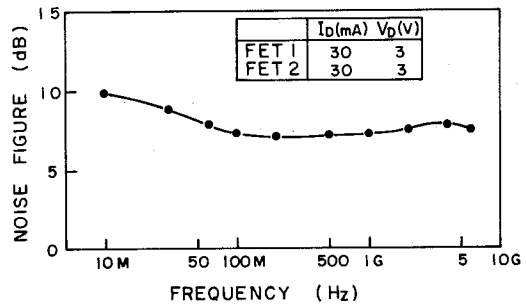


Fig. 13. Noise figure for the 800-kHz to 9.5-GHz amplifier module.

the output waveform  $t_o$  is given by

$$t_a^2 \approx t_o^2 - t_i^2. \quad (3)$$

Using above relation,  $t_a$  is calculated as 40 ps. There is another approximate relation between amplifier high-cut-off frequency  $f_c$  and  $t_a$ , as

$$f_c t_a \approx \frac{1}{3}. \quad (4)$$

From this relation,  $t_a = 35$  ps is estimated. Results from (3) and (4) are in good agreement.

Fig. 12(c) shows a measured step response for the cascade amplifier, where the input waveform is the same as in Fig. 12(a).  $t_a$  is estimated as 50 ps. No serious rise time degradation in the cascade amplifier is observed. This can also be predicted from the gain-frequency characteristic for the cascade amplifier.

### C. Noise

Since the developed amplifier module has 12-dBm power output at 1-dB gain compression, it can be used as a main amplifier in some systems. Noise characteristics matter little for main amplifiers. However, when using the amplifier module as a preamplifier, its noise figure (NF) is very important. Also, it has been reported that GaAs FET's have  $1/f$  noise below several hundred megahertz [5]. Accordingly, noise characteristics for the 800-kHz to 9.5-GHz amplifier module were measured.

Fig. 13 shows the NF over the 10-MHz to 6-GHz range. Better than 8-dB NF was observed across the 50-MHz to 6-GHz range. As shown in the figure, NF has a  $-0.8$  dB/octave slope across the 10-MHz to 50-MHz range.

To observe the noise characteristics below 10 MHz, output noise spectra for the amplifier module were measured using the spectrum analyzer. Fig. 14(a) shows the output noise spectra under bias supplied condition. Fig. 14(b) shows the output noise spectra without bias supply. As seen, amplifier output noise spectra have a  $-3$  dB/octave slope below 4 MHz. This shows the existence of amplifier  $1/f$  noise below 4 MHz. The NF variation caused by  $\pm 33$ -percent drain current variation was within  $\pm 0.1$  dB.

In the amplifier module, parallel 50- $\Omega$  resistor  $R_1$  in Fig. 2 is used to reduce input VSWR in the low-frequency range. However, this resistor degrades the amplifier NF in

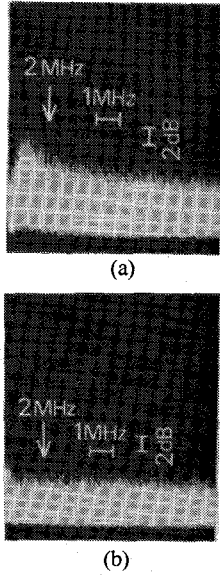


Fig. 14. Noise spectra for the 800-kHz to 9.5-GHz amplifier module. (a) With bias supply. (b) Without bias supply.

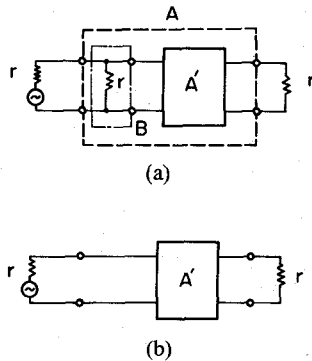


Fig. 15. Block diagram for NF explanation. (a) With parallel resistor. (b) Without parallel resistor.

the low-frequency range. To explain the magnitude of the NF degradation by  $R_1$ , Fig. 15 is presented. As shown in Fig. 15(a), amplifier module A is divided into two sections  $A'$  and B. NF ( $F$ ) of section  $A'$  is given by [6]

$$F = F_0 + \frac{R_n}{(2/r)} \left[ \left( \frac{2}{r} - G_0 \right)^2 + B_0^2 \right] \approx 2 \cdot \frac{R_n}{r} \quad (5)$$

where minimum NF for section  $A'$  is  $F_0$ , and source admittance, which gives  $F_0$  is  $Y_0 = G_0 + jB_0$ .  $R_n$  is the equivalent noise resistance for section  $A'$ . NF ( $F'$ ) for amplifier module A is given by

$$F' = F_B + \frac{F-1}{G_{av}} = 2 \cdot F \approx 4 \cdot \frac{R_n}{r} \quad (6)$$

where  $F_B$  is the NF for section B ( $F_B = 2$ ) and  $G_{av}$  is the available gain in section B ( $G_{av} = \frac{1}{2}$ ). Meanwhile, the NF for amplifier  $A'$  in Fig. 15(b) is given by

$$F'' = F_0 + \frac{R_n}{(1/r)} \left[ \left( \frac{1}{r} - G_0 \right)^2 + B_0^2 \right] \approx \frac{R_n}{r} \quad (7)$$

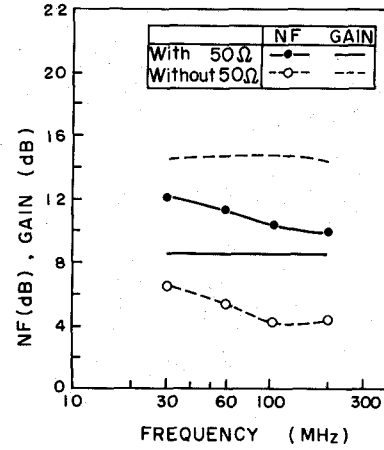


Fig. 16. NF degradation caused by parallel resistor.

Assuming  $F_0 \ll (R_n/r)$ ,  $(1/r) \gg G_0$ , and  $1/r \gg B_0$ , which is reasonable for source grounded GaAs FET's in the low-frequency range, NF ratio  $F'/F''$  is approximated as

$$\frac{F'}{F''} \approx \frac{4R_n/r}{1R_n/r} = 4. \quad (8)$$

Consequently, the addition of section B causes nearly 6-dB NF degradation. To validate the result, NF values for the second 800-kHz to 9.5-GHz amplifier module, with and without  $R_1$ , were measured. As shown in Fig. 16, amplifier NF and gain without  $R_1$  are about 6 dB better than amplifier NF and gain with  $R_1$ . However, input VSWR without  $R_1$  becomes large.

Consequently, circuit configuration, which requires no parallel resistor, should be considered if NF is a matter of concern.

### V. CONCLUSIONS

A novel ultrabroad-band amplifier design technique has been developed. The developed amplifier circuit operates as a C-R coupled amplifier circuit in the low-frequency range. It also utilized a lossless matching circuit in the microwave frequency range. Using this design method, an 800-kHz to 9.5-GHz bandwidth (13.5 octaves) amplifier module with 8.6-dB gain has been realized. The amplifier module has 40-ps step response rise time. It also has low input and output VSWR. By cascading two amplifier modules, 19-dB gain over the 800-kHz to 8.5-GHz range and 50-ps step response rise time were obtained. It was demonstrated that, by cascading the modules, higher gain can be obtained without degrading the bandwidth and the rise time. NF for the amplifier module is better than 8 dB over the 50-MHz to 6-GHz range.

The design examples presented in this paper have a simple circuit configuration. By increasing number of matching circuit sections and transformer sections, and by using shorter gate length FET's, wider bandwidth can be realized.

## ACKNOWLEDGMENT

The authors would like to thank H. Kohzu for supplying GaAs FET's. They would also like to thank K. Ayaki and H. Katoh for their constant encouragement throughout this work.

## REFERENCES

- [1] D. Hornbuckle, "GaAs IC direct-coupled amplifiers," in '80 *MTT-S Int. Microwave Symp. Dig. Tech. Papers*, pp. 387-389, May 1980.
- [2] R. V. Tuyle, "A monolithic integrated 4-GHz amplifier," in '78 *Int. Solid-State Circuits Conf., Dig. Tech. Papers*, pp. 72-73, Feb. 1978.
- [3] H. Q. Tserng and H. M. Macksey, "Ultra-wideband medium-power GaAs MESFET amplifiers," in '80 *Int. Solid-State Circuits Conf., Dig. Tech. Papers*, pp. 166-167, Feb. 1980.
- [4] K. B. Niclas, W. T. Wilser, R. B. Gold, and W. R. Hitchens, "A 350 MHz-14 GHz MESFET amplifier using feedback," in '80 *Int. Solid-State Circuits Conf., Dig. Tech. Papers*, pp. 164-165, Feb. 1980.
- [5] C. P. Snapp, "Microwave bipolar transistor Technology-present and prospects," in *9th European Microwave Conf. Proc.*, pp. 3-12, Sep. 1979.
- [6] W. R. Atkinson *et al.* "Representation of noise in linear twoports," *Proc. IRE*, vol. 48, pp. 69-74, Jan. 1960.

# Reliability of Power GaAs FET's—Au Gates and Al–Au Linked Gates

ELIOT D. COHEN, SENIOR MEMBER, IEEE, ALAN C. MACPHERSON, SENIOR MEMBER, IEEE, AND ARISTOS CHRISTOU, MEMBER, IEEE

**Abstract**—An investigation of the reliability of two types of commercial microwave power GaAs FET's has been carried out. Mean-time-to-failure data for a device mounted face-up with Al gates but without an Al–Au couple is presented and similar data for a "flip-chip" mounted Au-refractory gate device is reviewed. The failure mechanisms for both devices are described.

## I. INTRODUCTION

FOR SOME TIME, the Naval Research Laboratory (NRL) has been engaged in assessing the reliability of power GaAs FET's [1], [4]. The devices discussed in this paper were selected for evaluation for two reasons: 1) they are commercially available; and 2) they represent two different approaches to obviating a "gate void" problem [1]–[3] which occurs in devices with direct coupling between Al gate pad and Au. Such devices have very short mean-time-to-failures (MTTF's) as has been reported previously [1].

A causal relationship has now been established between the Al–Au couple and void formation [1]–[3]. There are at least two solutions to this problem: 1) the use of Au-refractory gates; 2) the Al gate in combination with a refractory link so that Au and Al do not come in contact. The Microwave Semiconductor Corporation (MSC) has

chosen the first while Raytheon has chosen the second solution. Unfortunately, in the case of the Raytheon device, the "solution" has introduced a new failure mechanism. However, in both cases, the void problem does not appear as a failure mode.

Both types of devices tested, Raytheon LNC 832D FET's and MSC 88002 FET's, are fabricated on semi-insulating GaAs substrates with buffer layers between the substrate and active layer. They both also have ohmic contacts formed by depositing Au–Ge/Ni on an  $n^+$  layer. The Raytheon devices have one center-fed  $1 \times 500 \mu\text{m}$  Al gate stripe and produce a nominal power output of approximately 200 mW at X-band. A refractory barrier metal sandwich has been fabricated between the Al gate and Au bonding pad to eliminate a direct Al–Au connection.

The MSC devices have eight titanium–tungsten–gold (Ti–W–Au) gate stripes, each of  $1 \times 150\text{-}\mu\text{m}$  dimensions and yield a nominal 0.5 W of output power at X-band. These FET's are mounted in a "flip-chip" configuration. All of the Raytheon FET's and most of the MSC devices tested were supplied in delidded packages although a few of the MSC units were mounted in packages with covers.

## II. TEST CONDITIONS

Before the devices were subjected to temperature accelerated life testing under RF conditions, a number of dc parameters were measured. These always included the normal grounded source transfer characteristics. In addition, gate-source current–voltage ( $I$ – $V$ ) characteristics were always measured. The latter proved to be the best indication of physical changes in the devices under test.

Manuscript received December 2, 1980; revised February 16, 1981. This work was supported by the U.S. Naval Electronic Systems Command and the U.S. Naval Air Systems Command.

E. D. Cohen was with the U.S. Naval Research Laboratory, Washington, DC. He is now with the U.S. Naval Electronic Systems Command, Washington, DC.

A. C. Macpherson and A. Christou are with the U.S. Naval Research Laboratory, Washington, DC 20375.